HAMP Domain Structural Determinants for Signaling and Sensory Adaptation in Tsr, the *E. coli* Serine Chemoreceptor

Peter Ames, Qin Zhou[1] and John S. Parkinson*

Biology Department
University of Utah
Salt Lake City, Utah 84112

running title: HAMP determinants for signaling and adaptation

[1] Present address: Pathology Department, University of Utah School of Medicine, Salt Lake City, UT 84302

* Corresponding author:
mailing address: University of Utah, 257 South 1400 East, Salt Lake City, UT 84112
phone: (801) 581-7639
FAX: (801) 581-4668
E-mail: *parkinson@biology.utah.edu*

Key words: signal transduction, chemotaxis, chemoreceptor, histidine kinase

---

Abbreviations: MCP, methyl-accepting chemotaxis protein;
CW, clockwise;
CCW, counter-clockwise;
IPTG, isopropyl-β-D-thiogalactopyranoside;
AS1, AS1', AS2, AS2', amphiphilic HAMP helices;
MH1, MH1', MH2, MH2', methylation helices;

Summary

HAMP domains mediate input-output transactions in many bacterial signaling proteins. To clarify the mechanistic logic of HAMP signaling, we constructed Tsr-HAMP deletion derivatives and characterized their steady-state signal outputs and sensory adaptation properties with flagellar rotation and receptor methylation assays. Tsr molecules lacking the entire HAMP domain or just the HAMP-AS2 helix generated clockwise output signals, confirming that kinase activation is the default output state of the chemoreceptor signaling domain and that attractant stimuli shift HAMP to an overriding kinase-off signaling state to elicit counter-clockwise flagellar responses. Receptors with deletions of the AS1 helices, which free the AS2 helices from bundle-packing constraints, exhibited kinase-off signaling behavior that depended on three C-terminal hydrophobic residues of AS2. We conclude that AS2/AS2' packing interactions alone can play an important role in controlling output kinase activity. Neither kinase-on nor kinase-off HAMP deletion outputs responded to sensory adaptation control, implying that out-of-range conformations or bundle-packing stabilities of their methylation helices prevent substrate recognition by the adaptation enzymes. These observations support the previously proposed biphasic, dynamic-bundle mechanism of HAMP signaling and additionally show that the structural interplay of helix-packing interactions between HAMP and the adjoining methylation helices is critical for sensory adaptation control of receptor output.

Introduction

Motile *Escherichia coli* cells track chemical gradients with high sensitivity over wide concentration ranges [recently reviewed in (Hazelbauer *et al.*, 2008; Hazelbauer & Lai, 2010)]. Stimulus detection, amplification, and integration occur in an arrayed network of signaling complexes that contain transmembrane chemoreceptors (methyl-accepting chemotaxis proteins or MCPs), the signaling histidine kinase CheA, and CheW, which couples CheA activity to chemoreceptor control. In the absence of chemoattractant gradients, MCPs activate CheA, promoting frequent episodes of clockwise (CW) flagellar rotation and random changes in swimming direction. Binding of an attractant ligand to the periplasmic sensing domain of a receptor molecule down-regulates CheA bound to the cytoplasmic tip of the receptor (Fig. 1), promoting counter-clockwise (CCW) flagellar rotation and forward swimming. Subsequent sensory adaptation restores pre-stimulus behavior through changes in MCP methylation state, catalyzed by a dedicated methyltransferase (CheR) and methylesterase (CheB).

A 50-residue HAMP domain plays a key mechanistic role in transmembrane signaling by bacterial chemoreceptors. HAMP domains promote two-way conformational communication between the input and output domains of many bacterial signaling proteins, including sensor histidine kinases, adenylyl cyclases, MCPs, and phosphatases (Aravind & Ponting, 1999; Williams & Stewart, 1999). HAMP subunits contain two amphiphilic helices (AS1, AS2) joined by a nonhelical connector segment (CTR). These conserved structural elements probably organize into 4-helix bundles in homodimeric signaling proteins (Butler & Falke, 1998; Swain & Falke, 2007; Watts *et al.*, 2008), as suggested by several high-resolution HAMP structures (Hulko *et al.*, 2006; Airola *et al.*, 2010).

Studies of *E. coli* chemoreceptors and sensor kinases demonstrate that HAMP domains can be locked in kinase-activating or kinase-inhibiting output states by single amino acid replacements and by cysteine-targeted disulfide bonds (Parkinson, 2010). The gearbox (Hulko *et al.*, 2006) and scissors (Swain & Falke, 2007) models of HAMP signaling propose discrete kinase-on and kinase-off conformations that correspond to alternate packing arrangements or

UU IR Author Manuscript

pivoting motions of the HAMP helices. In contrast, the dynamic-bundle model proposes that signal state reflects the packing stabilities of the HAMP helices and adjoining output helices (Zhou *et al.*, 2009). Thus, two-state models predict that mutant HAMP domains produce altered outputs by shifting the equilibrium proportions of the native HAMP signaling states, whereas the dynamic-bundle model predicts less structural specificity to HAMP signaling: Non-native HAMP structures that influence the packing stabilities of the output helices should also produce altered output signals.

To explore the structural determinants of HAMP output states in the *E. coli* serine chemoreceptor, we characterized the signaling properties of Tsr molecules lacking various portions of the HAMP domain. Most HAMP deletions produced kinase-on outputs, the default Tsr signaling state, but some caused kinase-off outputs, indicating suppression of default kinase activity. Both output states were refractory to sensory adaptation: The mutant receptors failed to undergo adaptational modifications, and amino acid replacements at their methylation sites had no effect on their output signals. These results indicate that the HAMP domain plays a central role in enabling Tsr molecules to undergo adaptational modifications and to change their output signals in response to those modifications. Moreover, the lack of structural specificity in HAMP output control implies that overall packing stabiity of the methylation helices determines receptor signal state, rather than a specific HAMP-imposed conformation. These mechanistic features are consistent with the dynamic-bundle model of HAMP signaling (Zhou *et al.*, 2009).

Results

Deletion scan of the Tsr-HAMP domain

We constructed and characterized a series of Tsr receptors lacking various HAMP structural elements (Fig. 2). The mutant constructs were made in pRR53, a regulatable Tsr expression plasmid (Studdert & Parkinson, 2005), and tested for function in otherwise receptorless host strains, using tryptone soft agar chemotaxis assays. All HAMP deletion constructs abrogated Tsr function, but expressed Tsr proteins of the expected sizes (data not shown) at nominally wild-type levels (Table 1). In complementation tests against recessive Tsr ligand-binding lesions

UU IR Author Manuscript

(Ames *et al.*, 2008; Zhou *et al.*, 2009), all Tsr-HAMP deletion defects were dominant, implying that deletion-bearing subunits cannot contribute to signaling function in Tsr heterodimers (data not shown). Similarly, none of the deleted receptors regained function in cells containing wild-type Tar molecules (data not shown), suggesting an irreparable disruption of input-output communication in the Tsr-HAMP deletions. In contrast, one-third of Tsr-HAMP missense mutants with loss-of-function defects were rescuable by Tar (Ames *et al.*, 2008; Zhou *et al.*, 2009).

To assess *in vivo* CheA activation by the Tsr-HAMP deletion constructs, we measured the effects of the plasmid-encoded mutant receptors on the flagellar rotation patterns of host strains that had deletions of all chromosomal receptor genes. Receptorless strains cannot form CheA-activating ternary complexes and, therefore, cannot produce CW motor rotation. If a mutant receptor cannot activate CheA, the cells show exclusively CCW rotation, the default direction of motor rotation. The ability of each mutant receptor to generate CW signals (expressed as the percent of cell time spent in CW rotation) was measured in both adaptation-deficient [Δ*(cheRB)*] and adaptation-proficient [$(cheRB)^+$] host strains to determine whether the mutant receptor output was subject to sensory adaptation control.

The flagellar rotation tests revealed two general output patterns in the Tsr-HAMP deletion mutants (Fig. 2; Table 1). (i) Some mutant receptors produced little or no CW output in either tester host [Δ(216-222), Δ(220-226), Δ(224-230), Δ(216-230), Δ(214-233)]; (ii) all other mutant receptors generated over 40% CW output in both hosts [Δ(214-244), Δ(216-245), Δ(235-241), Δ(235-245), Δ(243-246), Δ(235-267), Δ(251-257), Δ(258-264), Δ(246-267), Δ(214-254), Δ(214-263), Δ(214-267)]. In contrast, wild-type Tsr produced high CW rotation (79%) in the adaptation-deficient host, where all receptor molecules have an unaltered (QEQE) residue pattern at the principal methylation sites, but much lower CW output (26%) in the adaptation-proficient host, where the receptor population is heterogeneously modified through reversible methylation and demethylation of adaptation sites, promoted by CheR and CheB, respectively. CheB also irreversibly deamidates Q residues to create additional methyl-accepting E residues at

adaptation sites. The adaptation-insensitive rotation patterns of all Tsr-HAMP deletion mutants indicate that they produce locked output signals, either kinase-off (CCW) or kinase-on (CW).

Control logic of Tsr-HAMP signaling

Tsr molecules deleted for most [Δ(214-254)] or all [Δ(214-263), Δ(214-267)] of the HAMP domain produced CW-biased signal outputs in both adaptation-deficient and adaptation-proficient genetic backgrounds (Fig. 3). The extent of CW output was greatest for the two largest HAMP deletions [Δ(214-263), Δ(214-267)], suggesting that the AS2 remnants (residues 255-263) in the Δ(214-254) construct might suppress CheA activation to some extent. Nevertheless, compared to wild-type Tsr, all three ΔHAMP constructs had substantially elevated CW outputs in *(cheRB)*$^+$ hosts, reflecting a lack of adaptation control over their signal output. To exclude the possibility that the CW outputs of these ΔHAMP receptors arose through a special phase relationship of the TM2 and MH1 helices at the deletion junction, we inserted glycine residues at the Δ(214-254) and Δ(214-267) junctions to alter their helical registers. The additional glycines had no effect on the CW output of these mutant receptors in Δ*(cheRB)* hosts (Table 1). These TsrΔHAMP behaviors support two important conclusions: (i) HAMP is not required to attain the CheA-activating (CW) state; rather, this must be the default, HAMP-independent output state of the Tsr kinase control module. (ii) To produce CCW responses to attractant stimuli, HAMP must actively override this CW default signaling state.

A role for HAMP in sensory adaptation control of output

The lack of CheR and CheB influence over TsrΔHAMP output (Fig. 3) could mean that the mutant receptors are impervious to adaptational modification or that their output is locked in the kinase-on state, regardless of such modifications. To test the former possibility, we expressed TsrΔ(214-267) molecules in *(cheRB)*$^+$ and Δ*(cheRB)* hosts and assessed their modification states by their electrophoretic mobilities in SDS-containing polyacrylamide gels (Fig. 4). In the Δ*(cheRB)* host, both wild-type and deleted Tsr molecules migrated as a single species, representing the QEQE modification state of the receptor (Fig. 4A). In hosts containing only one of the adaptation enzymes (either CheR or CheB), wild-type receptors underwent extensive

modification, whereas TsrΔHAMP molecules did not (Fig. 4A). In the *(cheRB)*$^+$ host containing both modification enzymes, wild-type Tsr molecules exhibited both slower-migrating (-SER) and faster-migrating (+SER) species, representing molecules that have undergone CheB-mediated deamidation and CheR-mediated methylation, respectively (Fig. 4B). In contrast, TsrΔ(214-267) molecules exhibited no apparent modification changes (Fig. 4B), either in the absence or presence of a serine stimulus, indicating that HAMP-deleted receptor molecules are poor substrates for both CheB and CheR. These results suggest that the HAMP domain plays an active role in enabling the methylation helices to serve as substrates for the sensory adaptation enzymes.

To determine whether adaptational modifications can influence the signaling properties of TsrΔHAMP, we constructed EEEE and QQQQ derivatives of TsrΔ(214-267) to mimic fully unmethylated and highly methylated receptor states, respectively. In a Δ*(cheRB)* host, the modified ΔHAMP receptors produced predominantly CW-biased flagellar rotation patterns, indistinguishable from one another and from the QEQE version of TsrΔ(214-267) (Table 1). Notably, the EEEE and QEQE versions of TsrΔ(214-267) activated CheA equally well (73% and 71% CW), whereas the EEEE version of wild-type Tsr was much less activating than its QEQE counterpart (27% versus 79% CW). These results demonstrate that the HAMP domain also plays an active role in modulating signal output in response to modification changes of the methylation helices that are produced by the sensory adaptation enzymes.

Most of the Tsr-HAMP partial deletion constructs also exhibited substantial CW outputs (Table 1). These included ΔAS1-CTR, ΔCTR, ΔCTR-AS2, and ΔAS2 constructs (examples in Fig. 5A). Like the TsrΔHAMP constructs, none of these mutant receptors responded appropriately to the sensory adaptation system: Their CW output was as high or higher in hosts containing CheR and CheB as it was in hosts lacking both adaptation enzymes (Fig. 2; Table 1). Moreover, these classes of mutant receptors were not appreciably modified by either enzyme (Fig. 5B; Table 2). Thus, disruption of the HAMP bundle through ablation of HAMP structural elements in many cases leads to default activation of the receptor-coupled CheA kinase, but

UU IR Author Manuscript

blocks action of the sensory adaptation enzymes and prevents mutational mimics of adaptational modifications from regulating that CW output.

Suppression of CW output by HAMP structural elements

Unlike the majority of Tsr deletion constructs, those lacking only the AS1 helix produced little or no CW output, either in the absence or presence of the CheR and CheB enzymes (Fig. 2; Table 1). This behavior implies that the CTR-AS2 portion of HAMP, when not constrained in a stable bundle, can override the CheA-activating default output state of Tsr. The CCW output of TsrΔAS1 receptors is reminiscent of the behavior caused by single amino acid changes at critical HAMP bundle-packing residues (Zhou *et al.*, 2011). Polar and charged replacements at hydrophobic positions in AS1 and in the N-terminal half of AS2, which presumably destabilize the HAMP bundle, shift output to a CCW state [designated CCW(B)] that differs from the one induced by attractant stimuli [designated CCW(A)] (Zhou *et al.*, 2011). Three C-terminal hydrophobic residues of AS2 (L256, M259, L263) play a key role in attaining the CCW(B) output state, most likely by interacting aberrantly when they are not constrained by the HAMP bundle (Zhou *et al.*, 2011). Many amino acid replacements, especially polar residues, at any of these C-terminal AS2 positions (designated AS2c residues) prevent access to the CCW(B) state, producing default CW output instead (Zhou *et al.*, 2011). Thus, lesions in AS2c residues are epistatic to CCW(B) lesions elsewhere in HAMP: Doubly mutant receptors exhibit CW signal output (Zhou *et al.*, 2011).

If the CCW output of TsrΔAS1 receptors represents the CCW(B) state, we reasoned that lesions in AS2c residues should restore CW output to a TsrΔAS1 receptor. Accordingly, we introduced individual AS2c amino acid replacements into TsrΔ(214-233) and examined the output patterns of the doubly mutant receptors. A nonhydrophobic amino acid replacement at any of the three functionally critical AS2c residues restored substantial CW output to TsrΔ(214-233), producing rotation patterns comparable to those of ΔAS2 and ΔHAMP constructs (Fig. 6). These findings suggest that hydrophobic residues L256, M259, and L263 in the C-terminal portion of AS2 together suppress CW output when freed from the HAMP bundle structure. However, an unconstrained AS2 helix alone is evidently not sufficient for CCW(B) output,

UU IR Author Manuscript

because receptors lacking the CTR segment in addition to the AS1 helix [Δ(214-244); Δ(216-245)] exhibited high CW outputs (Fig. 2; Fig. 5A; Table 1). Perhaps CTR residues must interact with the N-terminal portion of AS2 to potentiate the aberrant structural interactions of the AS2c residues that lead to CCW(B) output.

Adaptation and clustering defects of CCW(B) receptors

Like the CW-signaling Tsr-HAMP deletion constructs, TsrΔAS1 molecules did not undergo adaptational modification by CheR or CheB (Table 2). Moreover, when mutationally modified to EEEE or QQQQ, TsrΔ(214-233) receptors still failed to produce CW output (Table 1). These behaviors support the premise that a structurally intact HAMP bundle is critical for adaptational modification of receptors and for changing receptor output in response to such modifications.

CW-signaling receptors must form ternary complexes in order to activate the CheA kinase. Core signaling complexes require prior assembly of receptor trimers of dimers and, when subsequently networked, lead to formation of polar receptor clusters (Gosink *et al.*, 2011). Receptor molecules that cannot generate CW output could either be defective in assembling ternary signaling complexes or they could form signaling complexes that are conformationally locked in a kinase-inactive state. Both sorts of defects have been seen in HAMP missense mutants with CCW(B) outputs (Zhou *et al.*, 2011). CCW(B) receptors with the most structure-destabilizing lesions (*e.g.*, charged replacements at hydrophobic packing residues) failed to assemble ternary complexes, whereas those with less drastic structural perturbations (*e.g.*, a polar amino acid at a hydrophobic packing position) assembled ternary complexes, but could not activate CheA (Zhou *et al.*, 2011).

To assess ternary complex formation by ΔAS1 mutant receptors, we examined their ability to form cellular clusters observable with three fluorescently-tagged reporter proteins, YFP-CheZ, YFP-CheW, and YFP-CheR. The YFP-CheZ reporter reveals ternary signaling complexes by binding to $CheA_S$ subunits, an alternate *cheA* translation product (Smith & Parkinson, 1980; Cantwell *et al.*, 2003), whereas the YFP-CheW reporter is incorporated directly into receptor signaling complexes. The TsrΔ(214-233) receptor did not form clusters detectable with either

the YFP-CheZ or YFP-CheW reporter (Fig. S1), suggesting that ΔAS1 receptors may not be able to assemble ternary signaling complexes. Alternatively, they might assemble ternary complexes, but fail to organize them into macroscopic clusters. To assess receptor clustering ability directly, we tested TsrΔ(214-233) with the YFP-CheR reporter, which binds to a pentapeptide sequence at the C-terminus of Tsr molecules (Wu *et al.*, 1996; Shiomi *et al.*, 2002) (see Fig. 1). The TsrΔAS1 mutant receptor also failed to form clusters observable with the YFP-CheR reporter (Fig. S1), suggesting that its CCW(B) output stems from a defect in an early step of ternary complex and cluster assembly, possibly in the formation of trimers of dimers, which appear to be structural precursors of both signaling complexes and receptor clusters (Ames *et al.*, 2002; Studdert & Parkinson, 2004). In contrast, TsrΔHAMP constructs that generated CW output signals exhibited wild-type levels of receptor clustering with all three reporters (Fig. S1), as did the TsrΔAS1 receptors that regained CW output through introduction of an amino acid replacement in one of the AS2c residues (Fig. 6 and data not shown).

Discussion

Two-state models of chemoreceptor signaling

The signaling properties of Tsr and other chemoreceptors of the MCP family generally conform to two-state models involving kinase-on and kinase-off output states (Fig. 7A). Thus, the fraction of receptor signaling complexes in each output state determines the cell's swimming behavior. Chemoeffector stimuli elicit signaling changes by shifting receptors to the OFF or ON state: The OFF state has higher affinity for attractant ligands; the ON state has higher affinity for repellents. The sensory adaptation system restores the pre-stimulus proportions of ON and OFF signaling complexes through net modification changes at receptor adaptation sites: CheR-mediated methylation shifts receptor output toward the ON state; CheB-mediated deamidation and demethylation shifts output toward the OFF state (Fig. 7A).

The nature of HAMP signaling states that produce kinase-on and kinase-off outputs is still under debate. Structural (Hulko *et al.*, 2006; Airola *et al.*, 2010), *in vivo* crosslinking (Watts *et al.*, 2008; Watts *et al.*, 2011), and chimeric protein studies (Ferris *et al.*, 2011; Mondejar *et al.*,

UU IR Author Manuscript

2012; Airola *et al.*, 2013) of chemoreceptors have been interpreted in terms of discrete signaling states that correspond to alternative ON and OFF conformations of the four-helix HAMP bundle. These discrete-state models leave unspecified the mechanisms of HAMP output control and HAMP interactions with the sensory adaptation system in chemoreceptors.

Conserved sequence features of HAMP-containing proteins (Parkinson, 2010; Stewart & Chen, 2010) and extensive mutational analyses of Tsr (Ames *et al.*, 2008; Zhou *et al.*, 2009; Zhou *et al.*, 2011) have suggested a different signaling model in which the HAMP output states comprise conformational ensembles rather than specific bundle packing arrangements (Zhou *et al.*, 2009; Parkinson, 2010). This dynamic-bundle model proposes that a phase stutter connection between the HAMP and MH bundles couples their packing stabiities in structural opposition (Fig. 7A). Tight packing of the HAMP helices destabilizes packing of the MH bundle helices; conversely, tight packing of the MH helices destabilizes the HAMP bundle (Fig. 7B). Thus, the dynamic-bundle model predicts that attractant stimuli promote stable HAMP packing, whereas repellent stimuli destabilize the HAMP bundle. During sensory adaptation, methylation increases promote MH bundle packing, whereas deamidation and demethylation destabilize the MH bundle. The interplay of these structural forces in turn regulates the kinase control tip of the receptor, possibly through another structural inversion at the glycine hinge (Swain *et al.*, 2009) (Fig. 7A & B).

In addition to the physiological ON and OFF HAMP states, the current study provides evidence for two non-native, adaptation-insensitive HAMP signaling states: CW locked and CCW(B) locked (Fig. 7A). Whether these and/or the physiological signaling states represent discrete HAMP structures or conformational ensembles remains an open question. However, the existence of non-native output states produced by HAMP sub-structures is more mechanistically consistent with the dynamic-bundle model than with a static two-state model, as explained below.

UU IR Author Manuscript

Control logic of HAMP domain signaling

Tsr molecules with deletions of the CTR and/or AS2 HAMP elements produced CW output signals, indicative of high CheA kinase activity. This kinase-on behavior resembles that of soluble Tsr signaling fragments that lack a HAMP domain (Ames & Parkinson, 1994; Ames *et al.*, 1996) and demonstrates that HAMP is not essential for kinase activation by Tsr. Thus, kinase-off signaling responses to attractant stimuli most likely involve an active override of a default kinase-on state. Both chemotaxis receptors (MCPs) and sensor histidine kinases (Appleman & Stewart, 2003; Stewart & Chen, 2010), the two most prevalent classes of HAMP-containing transducers, appear to use an active kinase-off control logic (Parkinson, 2010).

Evidence for two kinase-on signaling states in Tsr

Given active kinase-off logic, HAMP structural changes that impair or destabilize that kinase-off state should shift Tsr output toward higher kinase activity (Fig. 7A). Indeed, an uncharged, polar amino acid replacement at any of the hydrophobic packing residues of the HAMP bundle leads to elevated kinase output, suggesting that loosened bundle packing, rather than a specific HAMP structure, is sufficient to enhance output kinase activity (Zhou *et al.*, 2011). CW-signaling receptors within the physiological operating range are good substrates for deamidation and demethylation, modifications that shift receptors toward the native kinase-off state (Fig. 7A). We suggest that enhanced packing of the MH bundle helices creates structural features, for example close apposition of receptor subunits, that favor CheB substrate recognition and disfavor CheR substrate recognition. CheB might, for example recognize its substrate sites through binding contacts to more than one helix in the MH bundle.

We propose that the CW locked outputs of TsrΔHAMP receptors fall along the same dynamic continuum, but outside the physiological operating range of MH-bundle packing stabilities (Fig. 7A). Perhaps in the absence of any structural input from a HAMP domain, the MH helices pack too tightly to permit recognition of substrate sites by either CheB or CheR (Fig. 7C). Another symptom of MH bundle packing that is unopposed by HAMP structural inputs

UU IR Author Manuscript

is that the mutant receptor outputs are locked; they do not respond to mutationally-imposed changes in adaptational modification state.

Evidence for two kinase-off output states in Tsr

Attractant binding drives receptor molecules to the native kinase-off state, designated CCW(A), making their MH bundles good substrates for CheR action during sensory adaptation (Fig. 7A). The dynamic-bundle model postulates that the CCW(A) state corresponds to a stabilized HAMP structure with a packing geometry like the *x-da* or *a-d* helix packing arrangements of Af1503 HAMP (Hulko *et al.*, 2006; Zhou *et al.*, 2009). In both of these bundle geometries, the AS2/AS2' helices have a packing register that is out-of-phase with that of the adjoining MH1 and MH1' helices. Thus, HAMP in this CCW(A) structural state would most likely destabilize packing of the MH bundle. We propose that loose packing of the methylation helices makes them good substrates for CheR-mediated methylation (Fig. 7C). Perhaps CheR requires an isolated or destabilized methylation helix for substrate recognition. Subsequent neutralization of the negatively charged methyl-accepting glutamate residues should enhance MH bundle packing (Starrett & Falke, 2005; Winston *et al.*, 2005), thereby driving receptors away from the CCW(A) state during sensory adaptation.

Tsr-HAMP lesions that mimic the attractant-induced CCW(A) signaling state are relatively rare, presumably because they entail stability-enhancing structural changes (Parkinson, 2010). However, lesions predicted to greatly destabilize the HAMP bundle, such as charged amino acid replacements at hydrophobic packing residues, also lead to kinase-off output (Zhou *et al.*, 2011). In the present study, Tsr molecules deleted for the AS1 HAMP helix exhibited similar signaling properties, implying that drastic disruption of the native HAMP bundle can lead to kinase-off output. This so-called CCW(B) state requires the three C-terminal hydrophobic packing residues of the AS2 helix. Nonpolar amino acid replacements at any of those three AS2 residues restored kinase-on output to TsrΔAS1 (Fig. 6). We propose that in the CCW(B) state, hydrophobic interactions between the C-terminal AS2/AS2' residues contribute to MH bundle packing stability, leading to a very stable MH bundle that cannot activate CheA and is a poor substrate for CheR and CheB modifications (Fig. 7A & C).

The interaction of C-terminal AS2/AS2' residues postulated for the CCW(B) signaling state in Tsr corresponds to the packing arrangement reported in the HAMP2 bundle in the Aer2 protein of *Pseudomonas aeruginosa* (Airola *et al.*, 2010). When transplanted to the aspartate receptor Tar of *E. coli*, the Aer2-HAMP2 domain produced kinase-off output, which was suggested to resemble the native, attractant-induced HAMP state, CCW(A) (Airola *et al.*, 2013). Airola *et al.* further propose that the CCW(A) and CCW(B) HAMP states of Tsr employ the same structural mechanism for output control, namely, destabilization of MH bundle packing (Airola *et al.*, 2013). Our results indicate otherwise. First, receptors in the CCW(B) output state have properties in common with CW locked receptors (similar structural lesions; refractory to CheR and CheB action; refractory to imposed adaptational modifications) that place them close together on a structural or dynamic continuum (Fig. 7A). In contrast, receptors in the CCW(B) state have only their kinase-off output in common with receptors in the CCW(A) state, which readily assemble ternary complexes, are good substrates for CheR, and respond to adaptational modification. Finally, the kinase domains in receptor signaling complexes imaged by cryo-electron microscopy have very different mobilities in the CCW(A) and CCW(B) states (Briegel *et al.*, 2013). Moreover, CheA domains in kinase-on signaling complexes exhibit intermediate mobilities (Briegel *et al.*, 2013). These results would seem to place the CCW(A) and CCW(B) kinase-off output states at opposite ends of the receptor dynamic range (Fig. 7).

Participation of the HAMP domain in sensory adaptation

Receptors with HAMP domains locked in the CW or CCW(B) states were not only refractory substrates for the CheR and CheB enzymes, but mutationally imposed adaptational modifications failed to alter their output activity. These aberrant behaviors suggest that the MH bundles in HAMP-mutant receptors can lie outside the normal structural range and that the wild-type HAMP domain plays an indispensable role in the adaptation process. Evidently, structural interplay between the methylation helices and HAMP domain is necessary for sensory adaptation control of receptor output. Perhaps the opposing packing forces postulated in the dynamic-bundle model maintain the methylation helices of MCPs in the correct structural or

stability range for the sensory adaptation system to operate. HAMP-containing signaling proteins that lack sensory adaptation capability, might operate over a much narrower dynamic range.

ACKNOWLEDGMENTS

This work was supported by research grant GM19559 from the National Institute of General Medical Sciences. The Protein-DNA Core Facility at the University of Utah receives support from National Cancer Institute grant CA42014 to the Huntsman Cancer Institute.

MATERIALS AND METHODS

Bacterial strains. All strains were isogenic derivatives of *E. coli* K-12 strain RP437 (Parkinson & Houts, 1982) and carried the following markers relevant to this study: UU1250 [Δ*aer-1* Δ*tsr-7028* Δ(*tar-tap*)*5201* Δ*trg-100*] (Ames *et al.*, 2002), UU1535 [Δ*aer-1* Δ(*tar-cheB*)*2234* Δ*tsr-7028* Δ*trg-100*] (Bibikov *et al.*, 2004), UU2567 [Δ*(tar-cheZ)4211* Δ*tsr-5547* Δ*aer-1* Δ*trg-4543*] (this work), UU2610 [Δ*aer-1* Δ(*tar-cheB*)*4346* Δ*tsr-5547* Δ*trg-4543*] (Zhou *et al.*, 2011), UU2611 [Δ*aer-1* Δ(*tar-cheR*)*4283* Δ*tsr-5547* Δ*trg-4543*] (Zhou *et al.*, 2011), UU2612 [Δ*aer*-1 Δ(*tar-tap*) *4530* Δ*tsr-5547* Δ*trg-4543*] (Zhou *et al.*, 2011). and UU2632 [Δ*aer-1* Δ(*tar-tap*)*4530* Δ*cheB4345* Δ*tsr-5547* Δ*trg-4543*] (Zhou *et al.*, 2011).

Plasmids. Plasmids used in this work were: pKG116, a derivative of pACYC184 (Chang & Cohen, 1978) that confers chloramphenicol resistance and has a sodium salicylate inducible expression/cloning site (Buron-Barral *et al.*, 2006), and pPA114, a relative of pKG116 that carries wild-type *tsr* under salicylate control (Ames *et al.*, 2002); pRR48, a derivative of pBR322 (Bolivar *et al.*, 1977) that confers ampicillin resistance and has an expression/cloning site with a *tac* promoter and an ideal (perfectly palindromic) *lac* operator under the control of a plasmid-encoded *lacI* repressor, inducible by isopropyl β-D-thiogalactopyranoside (IPTG) (Studdert & Parkinson, 2005), and pRR53, a derivative of pRR48 that carries wild-type *tsr* under IPTG control (Studdert & Parkinson, 2005).

Plasmids used in receptor clustering assays were: pVS49, a derivative of pACYC184 (Chang & Cohen, 1978) that makes a functional yellow fluorescent protein (YFP)-CheZ fusion protein under inducible arabinose control (Sourjik & Berg, 2000); pVS102, a relative of pVS49 that makes a functional YFP-CheR fusion protein under inducible arabinose control (Kentner *et al.*, 2006); and pPA801 a relative of pVS49 that makes a functional YFP-CheW fusion protein under inducible arabinose control (Mowery *et al.*, 2008).

Directed mutagenesis. Plasmid mutations were generated by QuikChange PCR mutagenesis as previously described (Ames *et al.*, 2002). We used complementary oligonucleotides in which the 18-21 bases upstream of the DNA sequence targeted for deletion were fused to the same

UU IR Author Manuscript

number of bases downstream of the targeted DNA sequence. All mutational changes were verified by sequencing the entire *tsr* coding region in the mutant plasmid.

Chemotaxis assays. Host strains carrying Tsr expression plasmids were assessed for chemotactic ability on tryptone soft agar plates (Parkinson, 1976) containing appropriate antibiotics (ampicillin [50 μg/ml] or chloramphenicol [12.5 μg/ml]) and inducers (100 μM IPTG or 0.6 μM sodium salicylate). Plates were incubated for 7 to 10 h at 30°C or 32.5°C.

Flagellar rotation assays. Flagellar rotation patterns of Tsr plasmid-containing cells were analyzed by antibody tethering as described previously (Slocum & Parkinson, 1985). We classified cells into 5 categories according to their pattern of flagellar rotation: exclusively CCW, CCW reversing, balanced CCW-CW, CW reversing, and exclusively CW. The fraction of CW rotation time for a population of tethered cells was computed by a weighted sum of each of the five rotation classes, as described (Ames *et al.*, 2002).

Expression levels of mutant Tsr proteins. Tsr expression from pRR53 and pPA114 derivatives was analyzed in strain UU1535 or UU2610 (to avoid multiple modification states) as described (Ames *et al.*, 2002).

Assay of receptor modification state. UU2610 or UU2612 cells harboring pRR53 derivatives encoding wild type Tsr or the TsrΔ(214-267) were grown in T-broth containing 50 μg/ml ampicillin and 100 μM IPTG at 30°C to mid-log phase. Cells from 2 ml of culture were pelleted by centrifugation, washed twice with KEP (10 mM K-PO_4, 0.01 mM K-EDTA, pH 7.0), concentrated 2-fold by resuspension in tethering buffer (Slocum & Parkinson, 1985) and divided into two 500 μl aliquots. Following incubation at 30°C for 20 min, L-serine (Sigma) was added to one aliquot to a final concentration of 10 mM, and incubation of both samples continued for 20 min. Cells were pelleted by centrifugation, and lysed by boiling in sample buffer (Laemmli, 1970). Tsr bands were resolved by SDS-PAGE, and visualized by immunoblotting as described (Mowery *et al.*, 2008).

Receptor clustering assays. Mutant pRR53 derivatives were introduced into UU2567 cells harboring pVS49, pVS102, or pPA801. Cells containing each pair of compatible plasmids were

UU IR Author Manuscript

grown in tryptone broth containing 50 μg/ml ampicillin and 12.5 μg/ml chloramphenicol. Tsr expression from pRR53 derivatives was induced with 100 μM IPTG; YFP-CheZ (pVS49) was induced with 0.005% L(+)-arabinose; YFP-CheR (pVS102) was induced with 0.01% L(+)-arabinose; YFP-CheW (pPA801) was induced with 0.004% L(+)-arabinose. Cells were grown at 30°C to mid-exponential phase and analyzed by fluorescence microscopy as previously described (Ames *et al.*, 2002; Mowery *et al.*, 2008).

Protein modeling and structural display. Atomic coordinates for the Tsr HAMP domain were generated from the Af1503 HAMP coordinates (PDB accession number 2ASW) as described (Ames *et al.*, 2008). Coordinates for Tsr HAMP threaded onto the Aer2-HAMP2 structure (Airola *et al.*, 2010) were generously provided by Mike Airola and Brian Crane (Cornell University). Structure images were prepared with MacPyMOL software (*http://www.pymol.org*).

REFERENCES

Airola, M., K. J. Watts & B. R. Crane, (2010) Structure of concatenated HAMP domains provides a mechanism for signal transduction. *Structure* **18**: 436-448.

Airola, M. V., N. Sukomon, D. Samanta, P. P. Borbat, J. H. Freed, K. J. Watts & B. R. Crane, (2013) HAMP domain conformers that propagate opposite signals in bacterial chemoreceptors. *PLoS Biol* **11**: e1001479.

Ames, P. & J. S. Parkinson, (1994) Constitutively signaling fragments of Tsr, the *Escherichia coli* serine chemoreceptor. *J. Bacteriol.* **176**: 6340-6348.

Ames, P., C. A. Studdert, R. H. Reiser & J. S. Parkinson, (2002) Collaborative signaling by mixed chemoreceptor teams in *Escherichia coli*. *Proc. Natl. Acad. Sci. USA* **99**: 7060-7065.

Ames, P., Y. A. Yu & J. S. Parkinson, (1996) Methylation segments are not required for chemotactic signalling by cytoplasmic fragments of Tsr, the methyl-accepting serine chemoreceptor of *Escherichia coli*. *Mol. Microbiol.* **19**: 737-746.

Ames, P., Q. Zhou & J. S. Parkinson, (2008) Mutational analysis of the connector segment in the HAMP domain of Tsr, the *Escherichia coli* serine chemoreceptor. *J. Bacteriol.* **190**: 6676-6685.

Appleman, J. A. & V. Stewart, (2003) Mutational analysis of a conserved signal-transducing element: the HAMP linker of the *Escherichia coli* nitrate sensor NarX. *J. Bacteriol.* **185**: 89-97.

Aravind, L. & C. P. Ponting, (1999) The cytoplasmic helical linker domain of receptor histidine kinase and methyl-accepting proteins is common to many prokaryotic signalling proteins. *FEMS Microbiol. Lett.* **176**: 111-116.

Bibikov, S. I., A. C. Miller, K. K. Gosink & J. S. Parkinson, (2004) Methylation-independent aerotaxis mediated by the *Escherichia coli* Aer protein. *J. Bacteriol.* **186**: 3730-3737.

Bolivar, F., R. Rodriguez, P. J. Greene, M. C. Betlach, H. L. Heyneker & H. W. Boyer, (1977) Construction and characterization of new cloning vehicles. *Gene* **2**: 95-113.

Briegel, A., P. Ames, J. C. Gumbart, C. M. Oikonomou, J. S. Parkinson & G. J. Jensen, (2013) The mobility of two kinase domains in the *Escherichia coli* chemoreceptor array varies with signalling state. *Mol. Microbiol.* **89**: 831-841.

Buron-Barral, M., K. K. Gosink & J. S. Parkinson, (2006) Loss- and gain-of-function mutations in the F1-HAMP region of the *Escherichia coli* aerotaxis transducer Aer. *J. Bacteriol.* **188**: 3477-3486.

Butler, S. L. & J. J. Falke, (1998) Cysteine and disulfide scanning reveals two amphiphilic helices in the linker region of the aspartate chemoreceptor. *Biochemistry* **37**: 10746-10756.

Cantwell, B. J., R. R. Draheim, R. B. Weart, C. Nguyen, R. C. Stewart & M. D. Manson, (2003) CheZ phosphatase localizes to chemoreceptor patches via CheA-short. *J. Bacteriol.* **185**: 2354-2361.

Chang, A. C. Y. & S. N. Cohen, (1978) Construction and characterization of amplifiable multicopy DNA cloning vehicles derived from the p15A cryptic miniplasmid. *J. Bacteriol.* **134**: 1141-1156.

Ferris, H. U., S. Dunin-Horkawicz, L. G. Mondejar, M. Hulko, K. Hantke, J. Martin, J. E. Schultz, K. Zeth, A. N. Lupas & M. Coles, (2011) The mechanisms of HAMP-mediated signaling in transmembrane receptors. *Structure* **19**: 378-385.

Gosink, K. K., Y. Zhao & J. S. Parkinson, (2011) Mutational analysis of N381, a key trimer contact residue in Tsr, the *Escherichia coli* serine chemoreceptor. *J. Bacteriol.* **193**: 6452-6460.

Hazelbauer, G. L., J. J. Falke & J. S. Parkinson, (2008) Bacterial chemoreceptors: high-performance signaling in networked arrays. *Trends. Biochem. Sci.* **33**: 9-19.

Hazelbauer, G. L. & W. C. Lai, (2010) Bacterial chemoreceptors: providing enhanced features to two-component signaling. *Curr. Opin. Microbiol.* **13**: 124-132.

Hulko, M., F. Berndt, M. Gruber, J. U. Linder, V. Truffault, A. Schultz, J. Martin, J. E. Schultz, A. N. Lupas & M. Coles, (2006) The HAMP domain structure implies helix rotation in transmembrane signaling. *Cell* **126**: 929-940.

Kentner, D., S. Thiem, M. Hildenbeutel & V. Sourjik, (2006) Determinants of chemoreceptor cluster formation in *Escherichia coli*. *Mol. Microbiol.* **61**: 407-417.

Laemmli, U. K., (1970) Cleavage of structural proteins during assembly of the head of bacteriophage T4. *Nature* **227**: 680-685.

Mondejar, L. G., A. Lupas, A. Schultz & J. E. Schultz, (2012) HAMP domain-mediated signal transduction probed with a mycobacterial adenylyl cyclase as a reporter. *J. Biol. Chem.* **287**: 1022-1031.

Mowery, P., J. B. Ostler & J. S. Parkinson, (2008) Different signaling roles of two conserved residues in the cytoplasmic hairpin tip of Tsr, the *Escherichia coli* serine chemoreceptor. *J. Bacteriol.* **190**: 8065-8074.

Parkinson, J. S., (1976) *cheA*, *cheB*, and *cheC* genes of *Escherichia coli* and their role in chemotaxis. *J. Bacteriol.* **126**: 758-770.

Parkinson, J. S., (2010) Signaling mechanisms of HAMP domains in chemoreceptors and sensor kinases. *Annu. Rev. Microbiol.* **64**: 101-122.

Parkinson, J. S. & S. E. Houts, (1982) Isolation and behavior of *Escherichia coli* deletion mutants lacking chemotaxis functions. *J. Bacteriol.* **151**: 106-113.

Shiomi, D., I. B. Zhulin, M. Homma & I. Kawagishi, (2002) Dual recognition of the bacterial chemoreceptor by chemotaxis-specific domains of the CheR methyltransferase. *J. Biol. Chem.* **277**: 42325-42333.

Slocum, M. K. & J. S. Parkinson, (1985) Genetics of methyl-accepting chemotaxis proteins in *Escherichia coli*: null phenotypes of the *tar* and *tap* genes. *J. Bacteriol.* **163**: 586-594.

Smith, R. A. & J. S. Parkinson, (1980) Overlapping genes at the *cheA* locus of *Escherichia coli*. *Proc. Natl. Acad. Sci. USA* **77**: 5370-5374.

Sourjik, V. & H. C. Berg, (2000) Localization of components of the chemotaxis machinery of *Escherichia coli* using fluorescent protein fusions. *Mol. Microbiol.* **37**: 740-751.

Starrett, D. J. & J. J. Falke, (2005) Adaptation mechanism of the aspartate receptor: electrostatics of the adaptation subdomain play a key role in modulating kinase activity. *Biochemistry* **44**: 1550-1560.

Stewart, V. & L. L. Chen, (2010) The S helix mediates signal transmission as a HAMP domain coiled-coil extension in the NarX nitrate sensor from *Escherichia coli* K-12. *J. Bacteriol.* **192**: 734-745.

Studdert, C. A. & J. S. Parkinson, (2004) Crosslinking snapshots of bacterial chemoreceptor squads. *Proc. Natl. Acad. Sci. USA* **101**: 2117-2122.

Studdert, C. A. & J. S. Parkinson, (2005) Insights into the organization and dynamics of bacterial chemoreceptor clusters through *in vivo* crosslinking studies. *Proc. Natl. Acad. Sci. USA* **102**: 15623-15628.

Swain, K. E. & J. J. Falke, (2007) Structure of the conserved HAMP domain in an intact, membrane-bound chemoreceptor: a disulfide mapping study. *Biochemistry* **46**: 13684-13695.

Swain, K. E., M. A. Gonzalez & J. J. Falke, (2009) Engineered socket study of signaling through a four-helix bundle: evidence for a yin-yang mechanism in the kinase control module of the aspartate receptor. *Biochemistry* **48**: 9266-9277.

Watts, K. J., M. S. Johnson & B. L. Taylor, (2008) Structure-function relationships in the HAMP and proximal signaling domains of the aerotaxis receptor Aer. *J. Bacteriol.* **190**: 2118-2127.

Watts, K. J., M. S. Johnson & B. L. Taylor, (2011) Different conformations of the kinase-on and kinase-off signaling states in the Aer HAMP domain. *J. Bacteriol.* **193**: 4095-4103.

Williams, S. B. & V. Stewart, (1999) Functional similarities among two-component sensors and methyl-accepting chemotaxis proteins suggest a role for linker region amphipathic helices in transmembrane signal transduction. *Mol. Microbiol.* **33**: 1093-1102.

Winston, S. E., R. Mehan & J. J. Falke, (2005) Evidence that the adaptation region of the aspartate receptor is a dynamic four-helix bundle: cysteine and disulfide scanning studies. *Biochemistry* **44**: 12655-12666.

Wu, J., J. Li, G. Li, D. G. Long & R. M. Weis, (1996) The receptor binding site for the methyltransferase of bacterial chemotaxis is distinct from the sites of methylation. *Biochemistry* **35**: 4984-4993.

Zhou, Q., P. Ames & J. S. Parkinson, (2009) Mutational analyses of HAMP helices suggest a dynamic bundle model of input-output signalling in chemoreceptors. *Mol. Microbiol.* **73**: 801-814.

Zhou, Q., P. Ames & J. S. Parkinson, (2011) Biphasic control logic of HAMP domain signalling in the *Escherichia coli* serine chemoreceptor. *Mol. Microbiol.* **80**: 596-611.

Table 1. Signal outputs of Tsr HAMP deletion mutants.

Tsr-HAMP deletion[a]	[Tsr][b]	%CW rotation time in host:[c]	
		Δ*(cheRB)*	*(cheRB)*$^+$
wild type			
QEQE	1.00	79 [5]	26 [5]
EEEE	0.80 [3]	27	28
QQQQ	0.65 [3]	58	24
ΔHAMP			
Δ(214-267)	0.90 [2]	71 [2]	73
+ Ω1G	0.70	70	nd
+ Ω3G	0.70	67	nd
+ EEEE	0.65	73 [2]	nd
+ QQQQ	0.95	64	nd
Δ(214-263)	0.60	55	67
Δ(214-254)	0.85	49	40
+ Ω2G	1.05	32	nd
ΔAS1			
Δ(216-222)[d]	2.85	22	0
Δ(220-226)	1.00 [4]	0	12
Δ(224-230)	1.25 [3]	1 [2]	0 [2]
Δ(216-230)	1.15 [4]	3	9
Δ(214-233)	0.80 [3]	1	3
+ EEEE	0.70	4	nd
+ QQQQ	0.55	2	nd
ΔAS1-CTR			
Δ(214-244)	0.90	68	90
Δ(216-245)	1.05 [2]	82	88
ΔCTR			
Δ(235-241)	0.75 [2]	72	60 [2]
Δ(235-245)[d]	6.95 [2]	69	80
Δ(243-246)	1.25 [2]	87	93
ΔCTR-AS2			
Δ(235-267)	1.35 [4]	53	49

Table 1. (continued)

ΔAS2			
Δ(251-257)	1.30 [2]	49	53
Δ(258-264)	0.85 [2]	46	42
Δ(246-267)	0.95 [2]	43	69 [2]

[a] These *tsr* deletions and their derivatives were constructed and characterized in plasmid pRR53.

[b] Steady-state levels of the mutant proteins (rounded to the nearest 0.05 value) relative to that of wild-type Tsr (QEQE form). Means are given for multiple determinations; square brackets indicate the number of independent measurements made. See Methods for measurement details; nd: not determined.

[c] CW rotation times were calculated from flagellar rotation profiles, as described in Methods; nd: not determined.

[d] These mutant proteins slowed cell growth, most likely due to above-normal expression levels at standard induction conditions (100 μM IPTG).

UU IR Author Manuscript

Table 2. Adaptational modification tests of Tsr-HAMP deletion mutants.

Tsr-HAMP deletion	modified by:[a] CheB	CheR	+SER methylation increase[b]
wild type			
QEQE	+	+	YES
EEEE	–	+	YES
QQQQ	+	–	YES
ΔHAMP			
Δ(214-267)	–	–	NO
ΔAS1			
Δ(216-222)	+/-	–	NO
Δ(220-226)	–	–	NO
Δ(216-230)	–	–	NO
Δ(214-233)	+/-	–	NO
ΔAS1-CTR			
Δ(216-245)	+/-	–	NO
ΔCTR			
Δ(235-245)	+/-	–	NO
Δ(243-246)	+/-	+/-	NO
ΔCTR-AS2			
Δ(235-267)	–	–	NO
ΔAS2			
Δ(246-267)	–	–	NO

[a] Modification of the mutant protein by CheB and CheR was assessed by band patterns in SDS-PAGE analyses of proteins made in hosts UU2611 and UU2632, respectively: no evident modification (-); some modification, but less extensive than for the wild-type protein (+/-); extent of modification comparable to wild-type (+); nd: not determined.

[b] Increase in methylation state induced by a serine stimulus in host UU2612.

FIGURE LEGENDS

Fig. 1 Tsr and HAMP domain architecture.

Left: Cartoon of the Tsr homodimer showing important signaling features. Cylindrical segments represent α-helical regions, drawn approximately to scale. Methylation sites shown as black circles indicate glutamine residues in native Tsr that must be deamidated to glutamates by CheB before accepting methyl groups; white circles represent native glutamate residues that are direct substrates for the CheR methyltransferase. The thickened region at the C-terminus of each subunit represents a pentapeptide sequence (NWETF) to which CheB and CheR bind.

Right: Structure of the Tsr HAMP domain modeled from the atomic coordinates for the HAMP domain of Af1503 (Hulko *et al.*, 2006). HAMP domain subunits form a parallel, 4-helix bundle. The AS1 helices (light gray) are joined to the AS2 helices (dark gray) by a non-helical connector (CTR).

Fig. 2 Primary structure of Tsr HAMP and output properties of Tsr HAMP deletions.

AS1 and AS2 hydrophobic residues that are critical for Tsr signaling function are highlighted in black (Zhou *et al.*, 2009); two critical hydrophobic residues in the connector are highlighted in gray (Ames *et al.*, 2008). White boxes enclose other functionally important Tsr-HAMP residues (Ames *et al.*, 2008; Zhou *et al.*, 2009; Zhou *et al.*, 2011). The extents of HAMP deletions characterized in this study are shown by dark horizontal bars labeled with the number of the first and last Tsr residue deleted. The deletion constructs are grouped and labelled at their right ends according to their missing HAMP structural elements. Their signal outputs, expressed as CW flagellar rotation time, in adaptation-deficient (UU1535; UU2610; dark gray bars) and adaptation-proficient strains (UU1250; UU2612; light gray bars) are summarized in the histograms at the right side of the figure.

Fig. 3 Signaling properties of Tsr wild-type and Tsr∆HAMP receptors. The flagellar rotation behaviors of cells expressing Tsr wild-type and Tsr-∆HAMP receptors were assigned to five categories, from exclusively CCW to exclusively CW (see Methods).

Rotation patterns obtained in Δ*(cheRB)* hosts (UU1535 and UU2610) are indicated with dark gray histogram bars; patterns obtained in *(cheRB)*$^+$ hosts (UU1250 and UU2612) are shown as light gray histogram bars. Rotation data for Tsr wild-type give the average and standard deviation for five independent experiments to show reproducibility of the assay.

Fig. 4 Modification patterns of Tsr wild-type and TsrΔ(214-267) receptors. Receptors expressed from plasmids in various host strains were analyzed by SDS-PAGE, as detailed in Methods. Marker bands indicate the positions of wild-type Tsr molecules in EEEE, QEQE, and QQQQ modification states. An unidentified, chromosomally-encoded, cross-reacting protein, present in all samples, runs very close to the Tsr-QQQQ position.

A. Steady-state modification patterns in strains UU2610 [Δ*(cheRB)*], UU2611 [Δ*(cheR)*], and UU2632 [Δ*(cheB)*].

B. Pre- and post-stimulus modification patterns in strain UU2612 [*(cheRB)*$^+$].

Fig. 5 Signaling properties and CheR/CheB modification of Tsr molecules with partial HAMP deletions.

A. Flagellar rotation patterns of cells expressing typical representatives of four HAMP partial deletion classes are shown. Dark gray histogram bars indicate rotation profiles in Δ*(cheRB)* hosts (UU1535 and UU2610); light gray bars indicate patterns in *(cheRB)*$^+$ hosts (UU1250 and UU2612). Table 1 lists the rotation behaviors produced by other examples of these partial HAMP deletion classes.

B. SDS-PAGE mobilities of mutant Tsr molecules expressed in different host strains: UU2610 (CheB$^-$ CheR$^-$); UU2611 (CheB$^+$ CheR$^-$); UU2612 (CheB$^+$ CheR$^+$); UU2632 (CheB$^-$ CheR$^+$)

Fig. 6 Signaling properties of TsrΔAS1 receptors. TsrΔ(214-233) produces exclusively CCW flagellar rotation in both a Δ*(cheRB)* host (dark gray bars) and a *(cheRB)*$^+$ host (light gray bars). The panels to the right show the rotation behaviors produced by derivatives of this ΔAS1 receptor with an amino acid replacement in any of the C-

terminal hydrophobic packing residues of AS2 (L256, M259, L263). The AS2c lesions shift the rotation profile toward more CW output, both in Δ(*cheRB*) hosts (dark gray bars) and in (*cheRB*)$^{+}$ hosts (light gray bars).

Fig. 7 Mechanistic interpretation of TsrΔHAMP signaling properties.

A. Dynamic-bundle model of HAMP output states. Arrows with white heads indicate structure-destabilizing effects; arrows with black heads indicate structure-stabilizing effects. Attractant stimuli enhance packing stability of the HAMP bundle, thereby destabilizing MH bundle packing and driving receptor signaling complexes to the kinase-off [CCW(A)] state. Repellent stimuli reduce HAMP packing stability, which enhances MH bundle stability and shifts receptors to a kinase-on (CW) output state. The sensory adaptation system offsets these signaling changes through methylation (black circles) and deamidation or demethylation (white circles) reactions, respectively catalyzed by CheR and CheB. Ablation of HAMP structural elements produces two non-physiological, adaptation-resistant output states: a kinase-on state (CW locked) and a kinase-off state [CCW(B) locked].

B. Opposed packing stabilities of the HAMP and MH bundles produced by a phase stutter joining the AS2 and MH1 helices. The dynamic-bundle model predicts that the four HAMP signaling states in (A) represent different local regions along this dynamic continuum.

C. Cross-sections of the MH bundle showing inter-helix packing interactions whose strength could provide a structural basis for feedback control of adaptational modifications. The loose packing forces (light gray lines) between MH helices in the CCW(A) (kinase-off) state may favor substrate site recognition by CheR, but disfavor substrate recognition by CheB. The tighter MH packing forces (gray lines) in the CW (kinase-on) state may reverse these substrate preferences. The even tighter packing forces (black lines) between MH helices in the locked CW and CCW(B) output states may preven substrate recognition by both CheR and CheB.

UU IR Author Manuscript

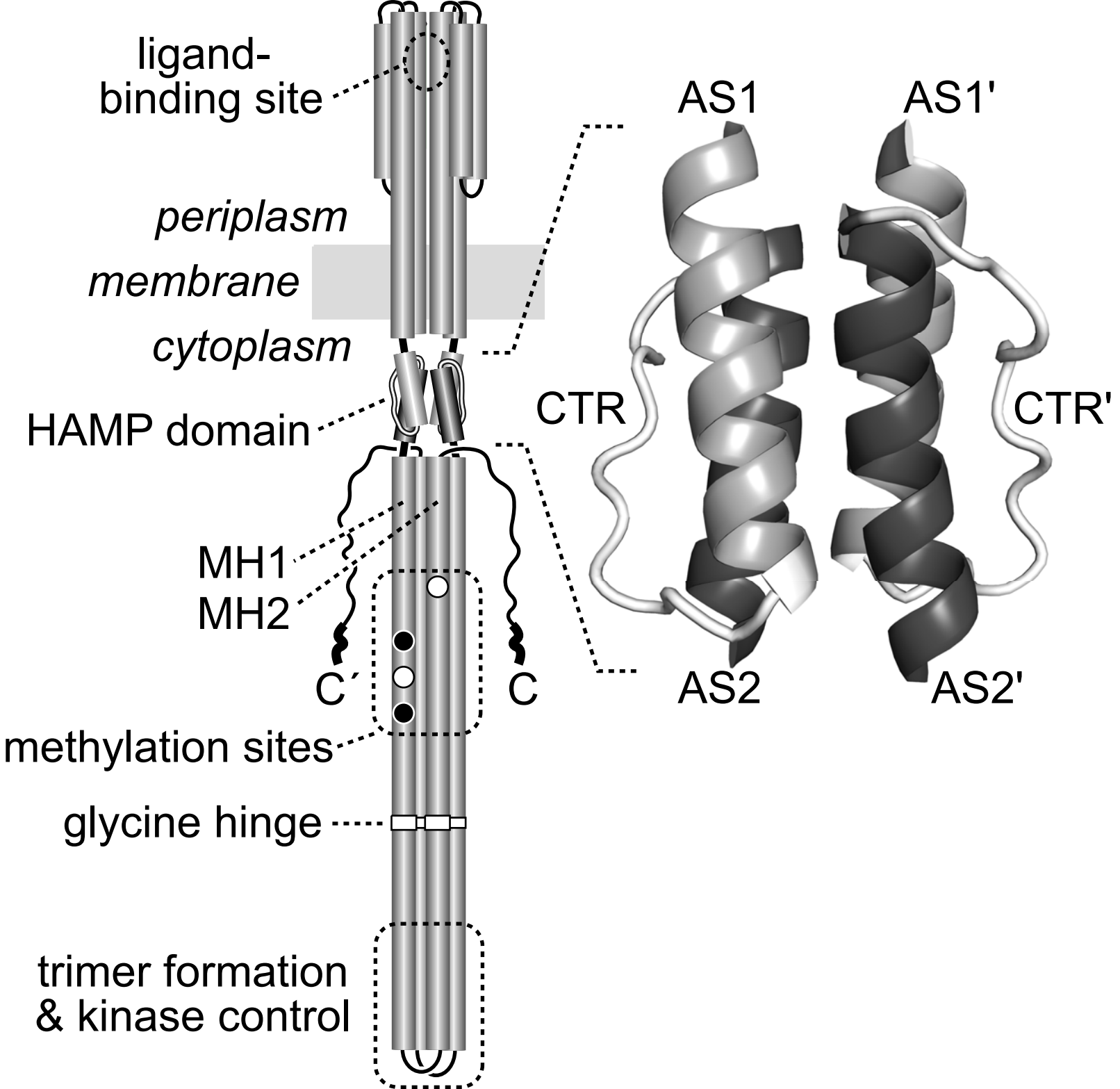
ligand-
binding site
periplasm
membrane
cytoplasm
HAMP domain
MH1
MH2
C´
C
methylation sites
glycine hinge
trimer formation
& kinase control
AS1
AS1'
CTR
CTR'
AS2
AS2'

HAMP

TM2 | control cable | AS1 | connector | AS2 | phase stutter | MH1

CW output
Δ(*cheRB*)
(*cheRB*)$^{+}$
0 100

211 212 213 214 215 216 217 218 219 220 221 222 223 224 225 226 227 228 229 230 231 232 233 234 235 236 237 238 239 240 241 242 243 244 245 246 247 248 249 250 251 252 253 254 255 256 257 258 259 260 261 262 263 264 265 266 267 268 269 270

• • W F G I K A S L V A P M N R L I D S I R H I A G G D L V K P I E V D G S N E M G Q L A E S L R H M Q G E L M R T V G D V • •

wild-type

Δ(216-222)
Δ(220-226)
Δ(224-230)
ΔAS1
Δ(216-230)
Δ(214-233)

Δ(214-244)
ΔAS1-CTR
Δ(216-245)

Δ(235-241)
Δ(235-245)
ΔCTR
Δ(243-246)

Δ(235-267)
ΔCTR-AS2

Δ(251-257)
Δ(258-264)
ΔAS2
Δ(246-267)

Δ(214-254)
Δ(214-263)
ΔHAMP
Δ(214-267)

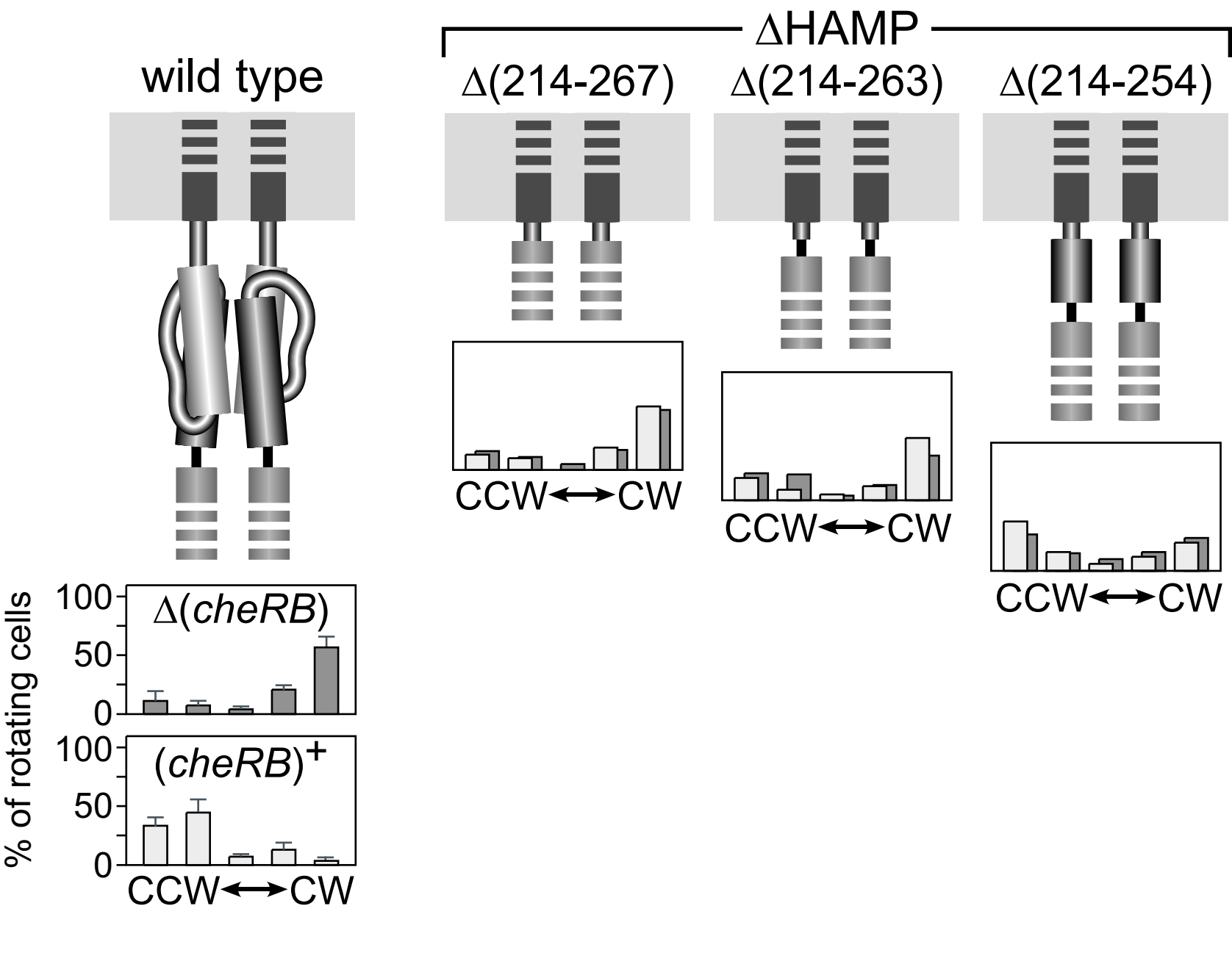
ΔHAMP
wild type
Δ(214-267)
Δ(214-263)
Δ(214-254)
CCW↔CW
CCW↔CW
CCW↔CW
% of rotating cells
100
50
0
Δ(cheRB)
100
50
0
(cheRB)+
CCW↔CW

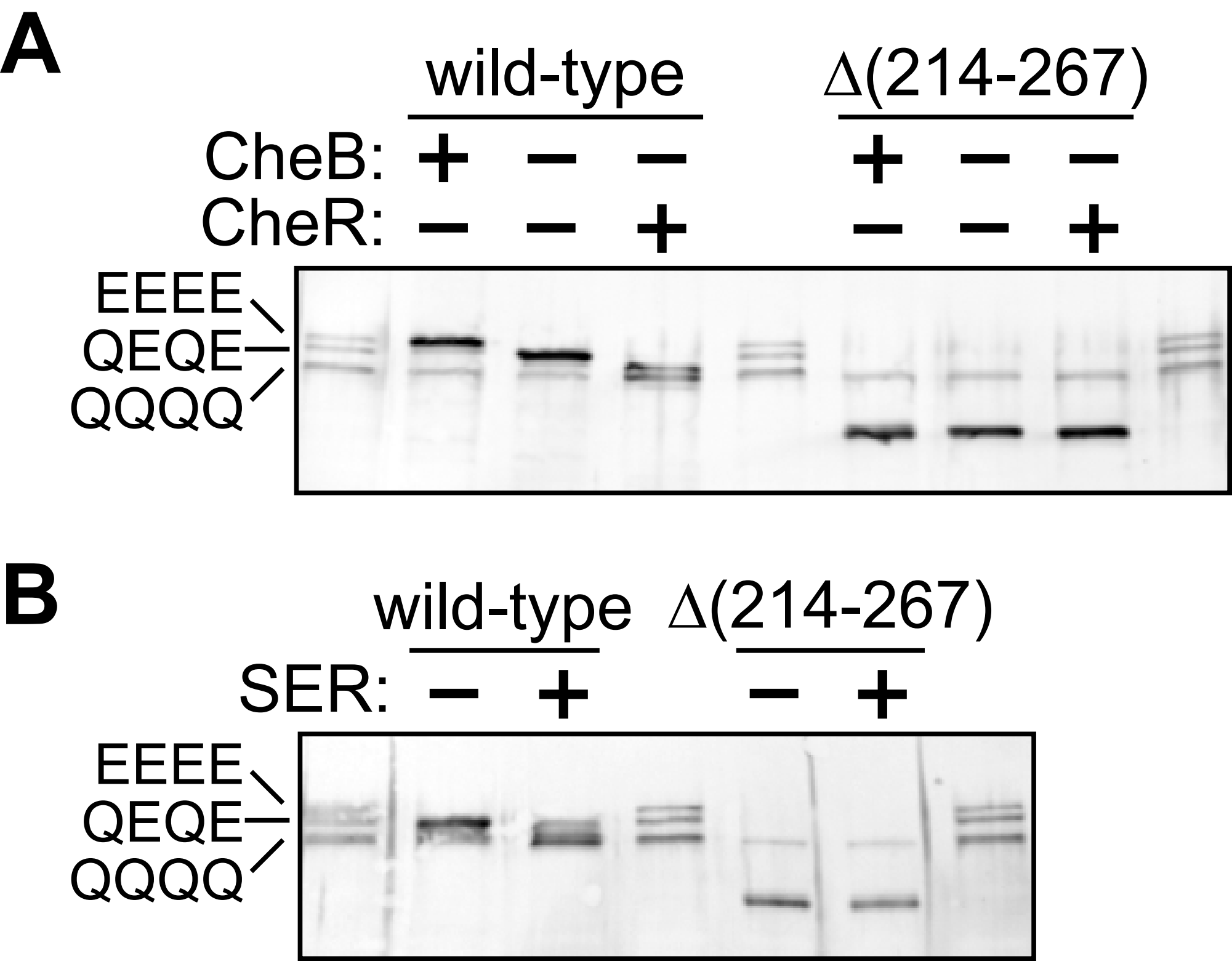
A
wild-type
Δ(214-267)
CheB: + − − + − −
CheR: − − + − − +
EEEE
QEQE
QQQQ
B
wild-type
Δ(214-267)
SER: − + − +
EEEE
QEQE
QQQQ

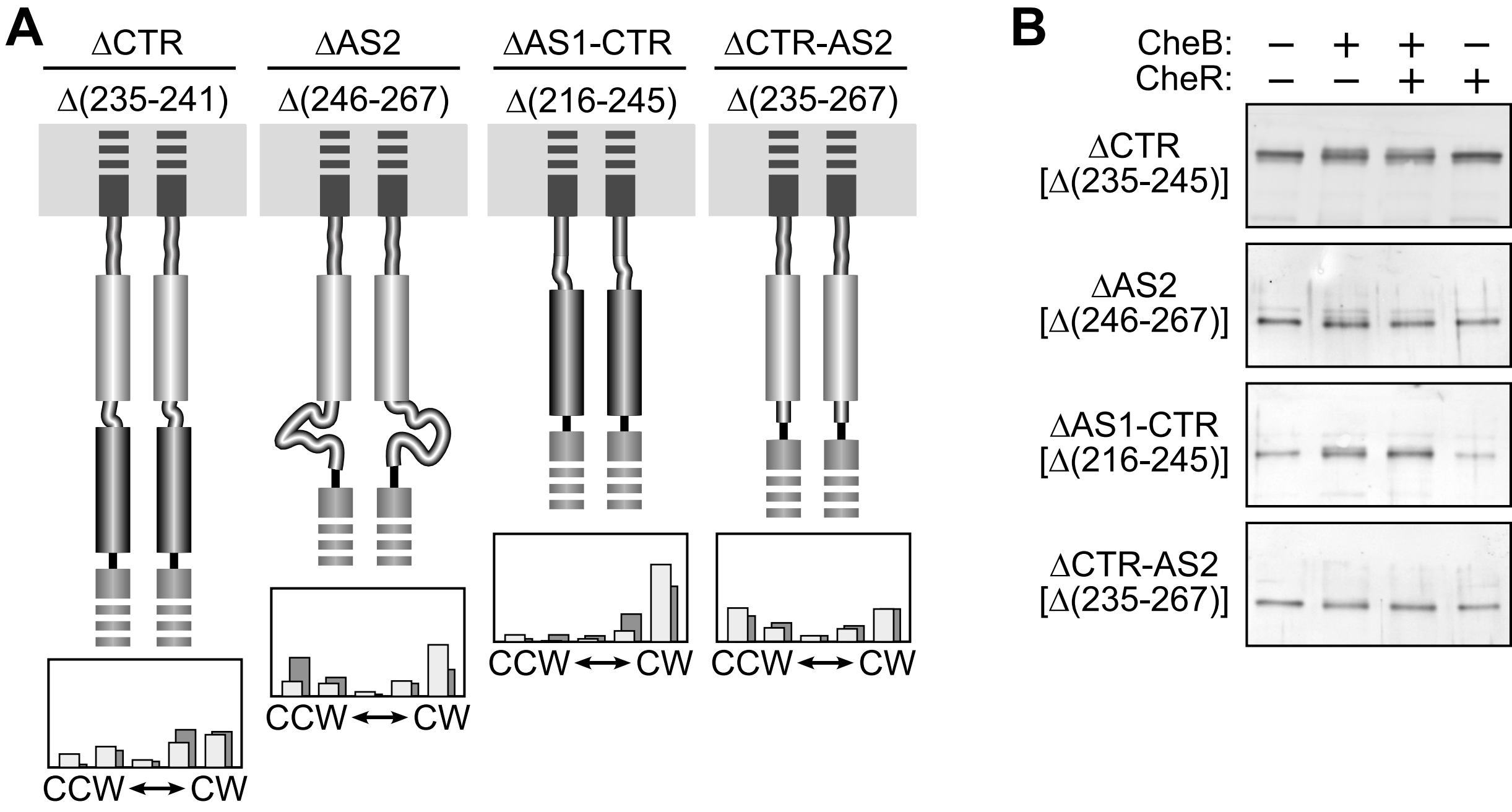
A
ΔCTR
Δ(235-241)
ΔAS2
Δ(246-267)
ΔAS1-CTR
Δ(216-245)
ΔCTR-AS2
Δ(235-267)
CCW ↔ CW
CCW ↔ CW
CCW ↔ CW
CCW ↔ CW
B
CheB: – + + –
CheR: – – + +
ΔCTR
[Δ(235-245)]
ΔAS2
[Δ(246-267)]
ΔAS1-CTR
[Δ(216-245)]
ΔCTR-AS2
[Δ(235-267)]

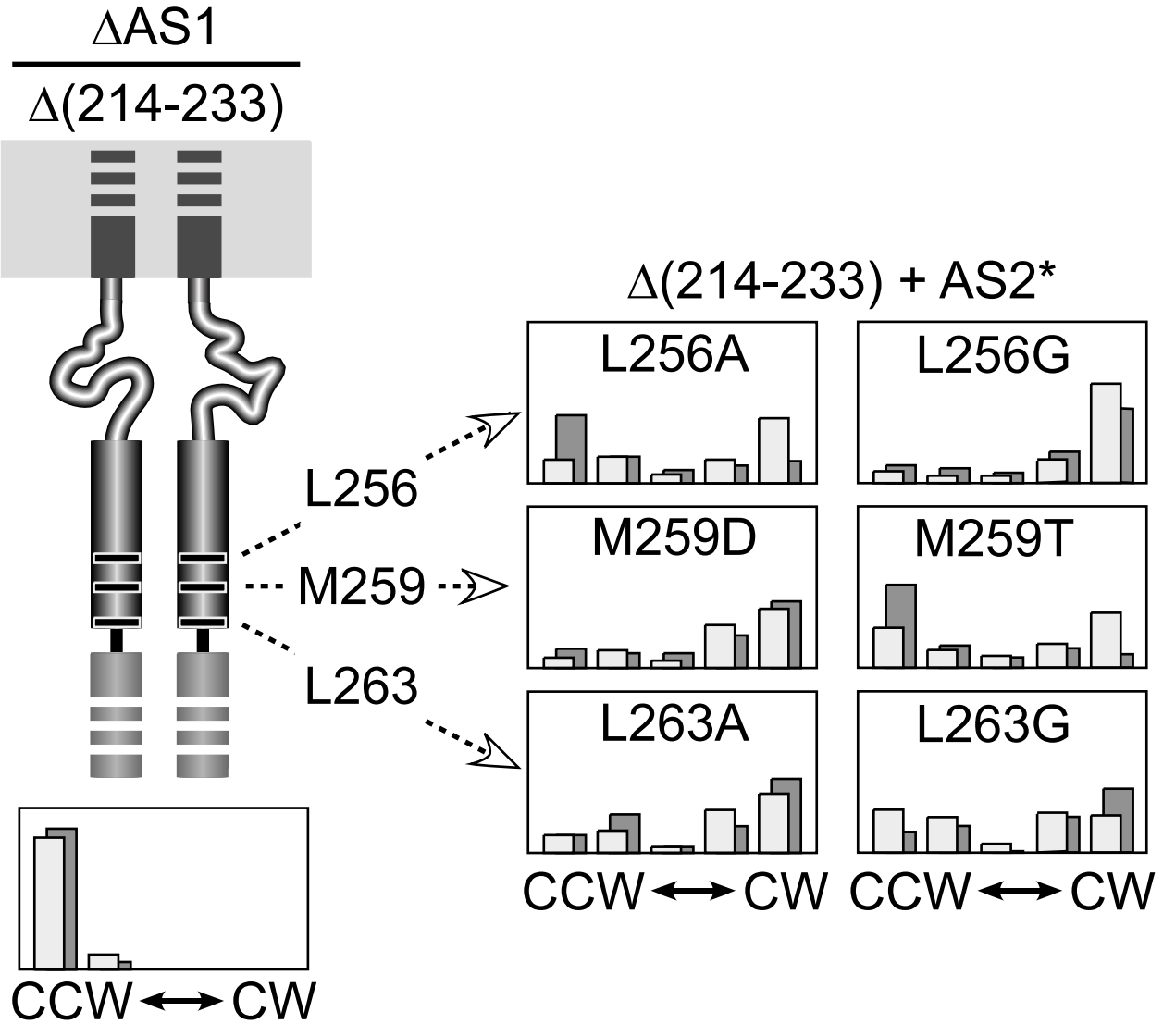
ΔAS1
Δ(214-233)
L256
M259
L263
Δ(214-233) + AS2*
L256A
L256G
M259D
M259T
L263A
L263G
CCW ↔ CW
CCW ↔ CW
CCW ↔ CW

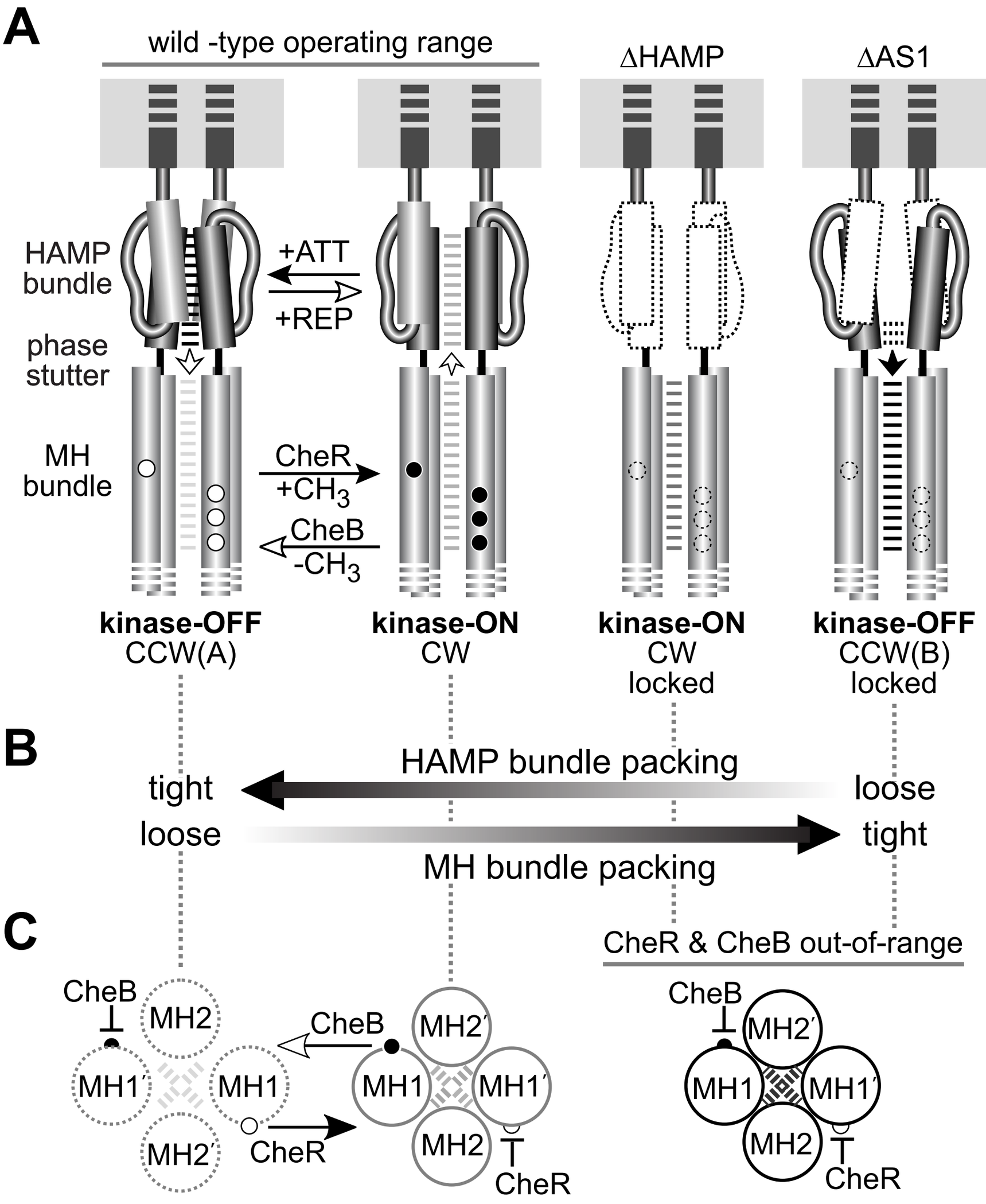
A
wild -type operating range
ΔHAMP
ΔAS1
HAMP bundle
phase stutter
MH bundle
+ATT
+REP
CheR +CH3
CheB -CH3
kinase-OFF CCW(A)
kinase-ON CW
kinase-ON CW locked
kinase-OFF CCW(B) locked
B
HAMP bundle packing
tight
loose
loose
tight
MH bundle packing
C
CheR & CheB out-of-range
CheB
MH2
MH1′
MH1
MH2′
CheR
MH2′
MH1
MH1′
MH2
CheR
CheB
MH2′
MH1
MH1′
MH2
CheR

Fig. S1 Clustering properties of Tsr wild-type and TsrΔHAMP receptors. Images were converted to grayscale and inverted so that receptor clusters appear as dark spots within the cells. Numbers in the center of each image indicate the percentage of at least 100 cells examined that had a discernable receptor cluster.